

# Measurements of stable carbon isotope ratio of methane at Hateruma Station, Japan

Taku Umezawa ([umezawa.taku@nies.go.jp](mailto:umezawa.taku@nies.go.jp)), Yukio Terao, Yasunori Tohjima, Takuya Saito, Motoki Sasakawa and Hitoshi Mukai

 National Institute for Environmental Studies

## Abstract

Hateruma island is the southernmost inhabited island of Japan. As the place is in the downwind of the continental East Asia in winter, arrivals of air masses of continental origin cause synoptic-scale variations (i.e., high-concentration events in CO<sub>2</sub>, CH<sub>4</sub> etc.). We have collected air samples so as to coincide with such high-CH<sub>4</sub> events, and those air samples have been analyzed for stable carbon isotope ratio of CH<sub>4</sub> ( $\delta^{13}\text{C-CH}_4$ ) since December 2017 by using a continuous-flow preconcentration and isotope ratio mass spectrometry system. In this study, we present our experimental method for  $\delta^{13}\text{C-CH}_4$  analysis including our attempts to assure data quality. We prepared a compressed dry air as a working standard as well as a set of three surveillance cylinders (CH<sub>4</sub> in synthetic air) that cover a wide range of  $\delta^{13}\text{C-CH}_4$  values (from -68 to -26 per mil VPDB). Two-year measurement records show that the three surveillance cylinders have indicated no significant drifts, and that the standard deviations of the measured values for the individual cylinders are about 0.1 per mil. It is also observed that the span of our  $\delta^{13}\text{C-CH}_4$  measurement (difference of the measured values of the cylinders with high and low  $\delta^{13}\text{C-CH}_4$ ) has been constant over time. Although temporal drift needs to be monitored for a longer period, we consider that performance of our system is satisfactory to identify synoptic-scale variations at Hateruma island and to infer  $\delta^{13}\text{C-CH}_4$  signatures of the continental CH<sub>4</sub> sources.

Table 1. Cylinder gases used for long-term quality assurance of  $\delta^{13}\text{C-CH}_4$  measurements at NIES.

| Gas Name | Cylinder ID | Composition  | $\delta^{13}\text{C-CH}_4$ (‰) |
|----------|-------------|--|--------------------------------|
| Work     | CPB03323    | Compressed dry air   | -47.49±0.13                    |
| LOW      | CC706220    | 2-ppm CH <sub>4</sub> + 1-ppm Kr in synthetic air (manufactured by Air Liquid) | -68.23±0.11                    |
| HIGH     | EB0132294   | 2-ppm CH <sub>4</sub> + 1-ppm Kr in synthetic air (manufactured by Air Liquid) | -26.88±0.09                    |
| MID      | EB0129050   | 2-ppm CH <sub>4</sub> + 1-ppm Kr in synthetic air (manufactured by Air Liquid) | -45.15±0.06                    |

## Measurement traceability

The  $\delta^{13}\text{C-CH}_4$  value of the working standard air (Work, **Table 1**) was determined based on replicated measurements during 9 November 2018–21 January 2019 ( $N=158$ ) against the reference CO<sub>2</sub> cylinder with  $\delta^{13}\text{C-CO}_2$  value of -32.46‰ (NIES VPDB). Work has been measured on every sample measurement day. Its  $\delta^{13}\text{C-CH}_4$  value has been assumed to be stable and sample measurements have been corrected accordingly.

## NIES $\delta^{13}\text{C-CH}_4$ measurement system

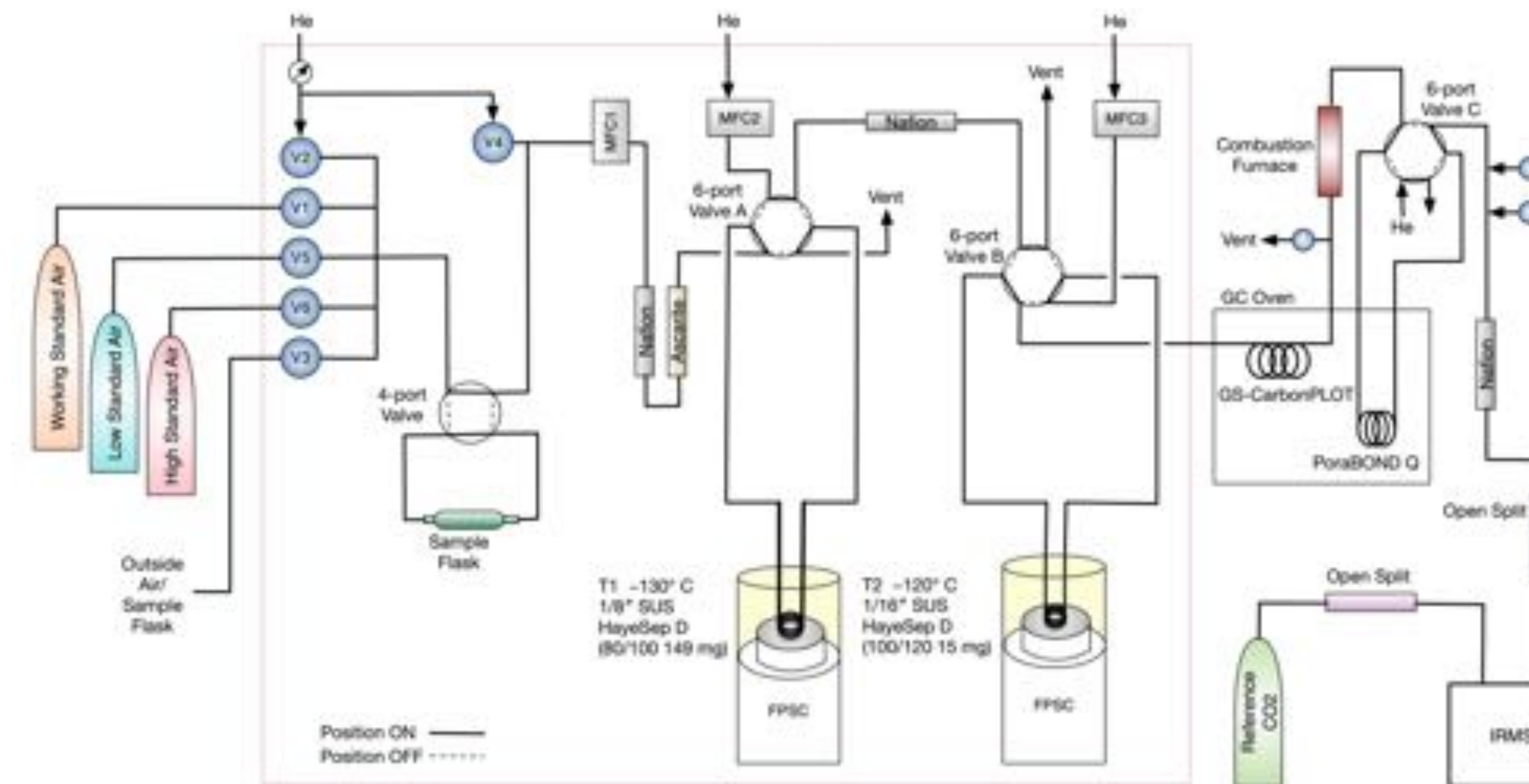


Figure 1. A schematic overview of the NIES CPR-GC-IRMS system. The sub-system CPR (Continuous-flow Preconcentration and Refocusing) is surrounded by the dotted square. The on/off valves V1 to V6, 4-port Valve and 6-port Valves A and B are controlled pneumatically by CPR. MFC: mass flow controller; IRMS: isotope ratio mass spectrometer. The figure has been modified after [Umezawa et al. \(2020\)](#).

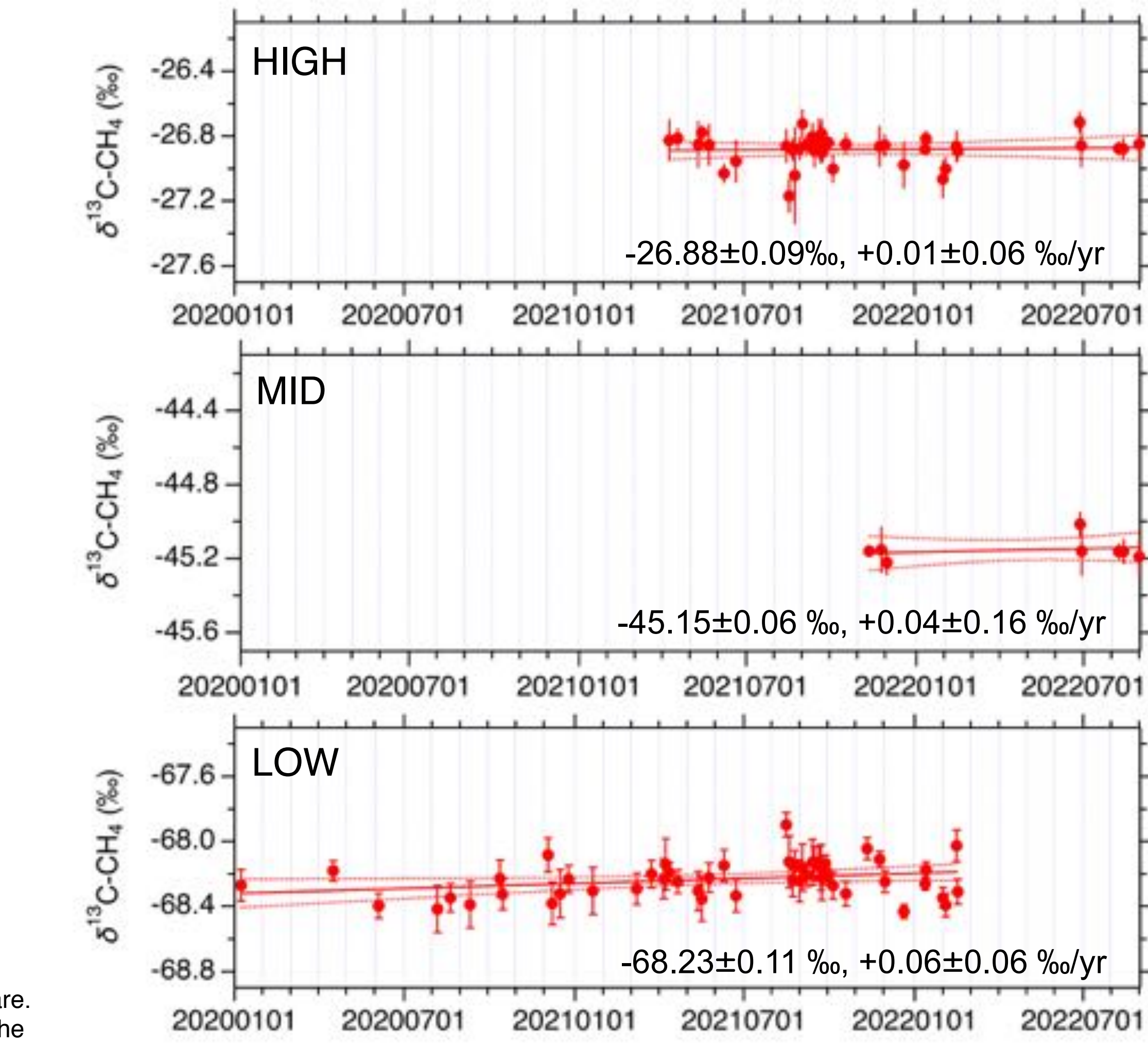


Figure 3. Time series of  $\delta^{13}\text{C-CH}_4$  measurements for the three surveillance cylinders: (top) HIGH, (middle) MID and (bottom) LOW. Average measurement values and time drifts are indicated (see also Table 1).

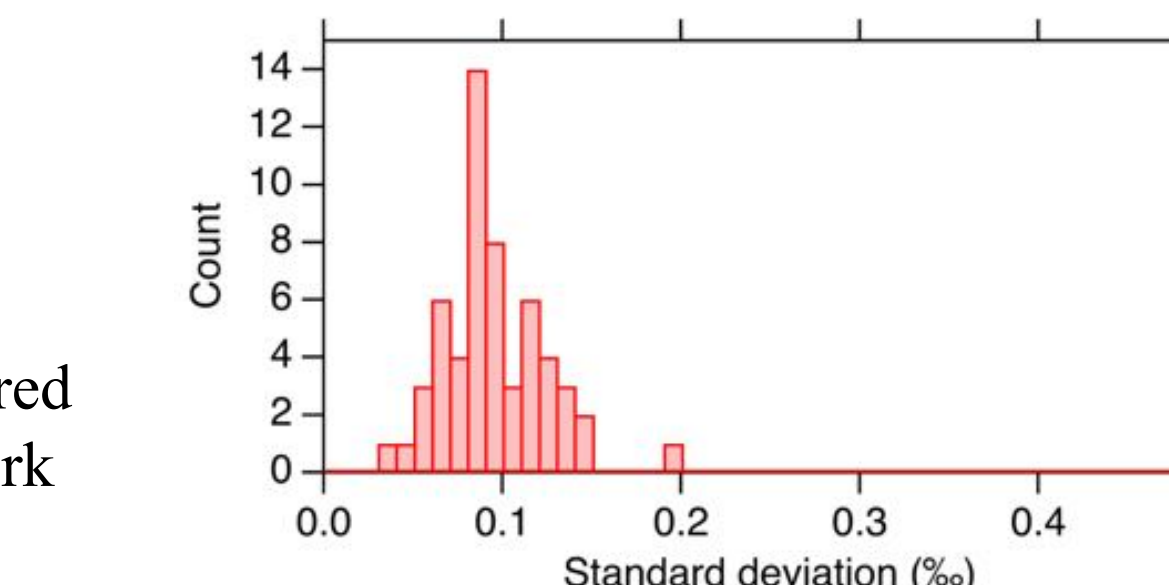


Figure 2. A histogram of standard deviation of the Work measurements on each measurement day during the periodic surveillance measurement series.

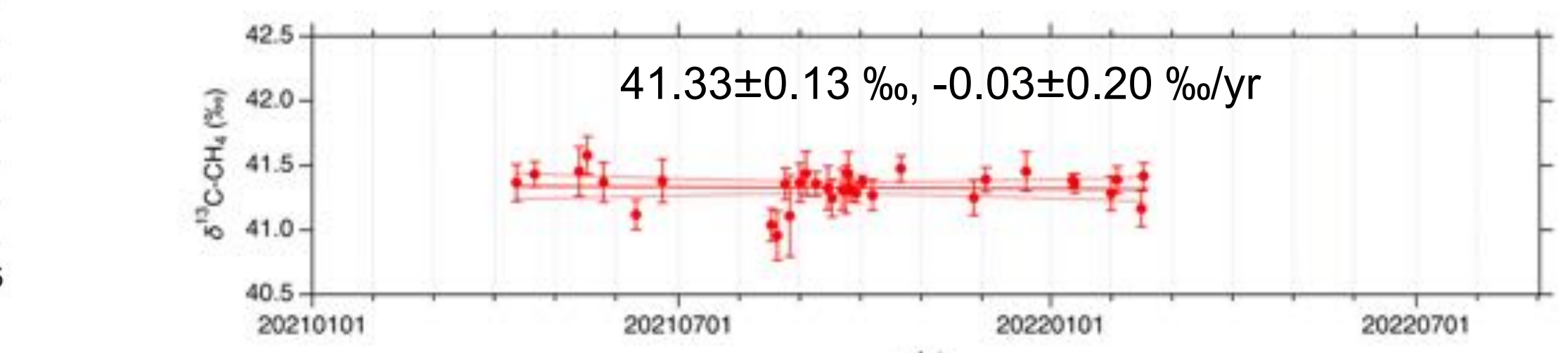


Figure 4. Time series of the measured  $\delta^{13}\text{C-CH}_4$  span (HIGH – LOW). Note that range of x-axis is different from Figure 3.

## Long-term quality assurance

Work and the three surveillance cylinders with wide range of  $\delta^{13}\text{C-CH}_4$  values (**Table 1**) are measured periodically in a replicate way (typically 10 times for each cylinder). Standard deviations of the Work measurements during those surveillance series are generally ~0.1‰ or better (Figure 2). The three surveillance cylinders did not show significant time drifts over the last two years (Figure 3). These measurements also indicate insignificant temporal change of the measurement span over the last years (Figure 4).

## Measurement results for air samples from the Hateruma Station (HAT), Japan

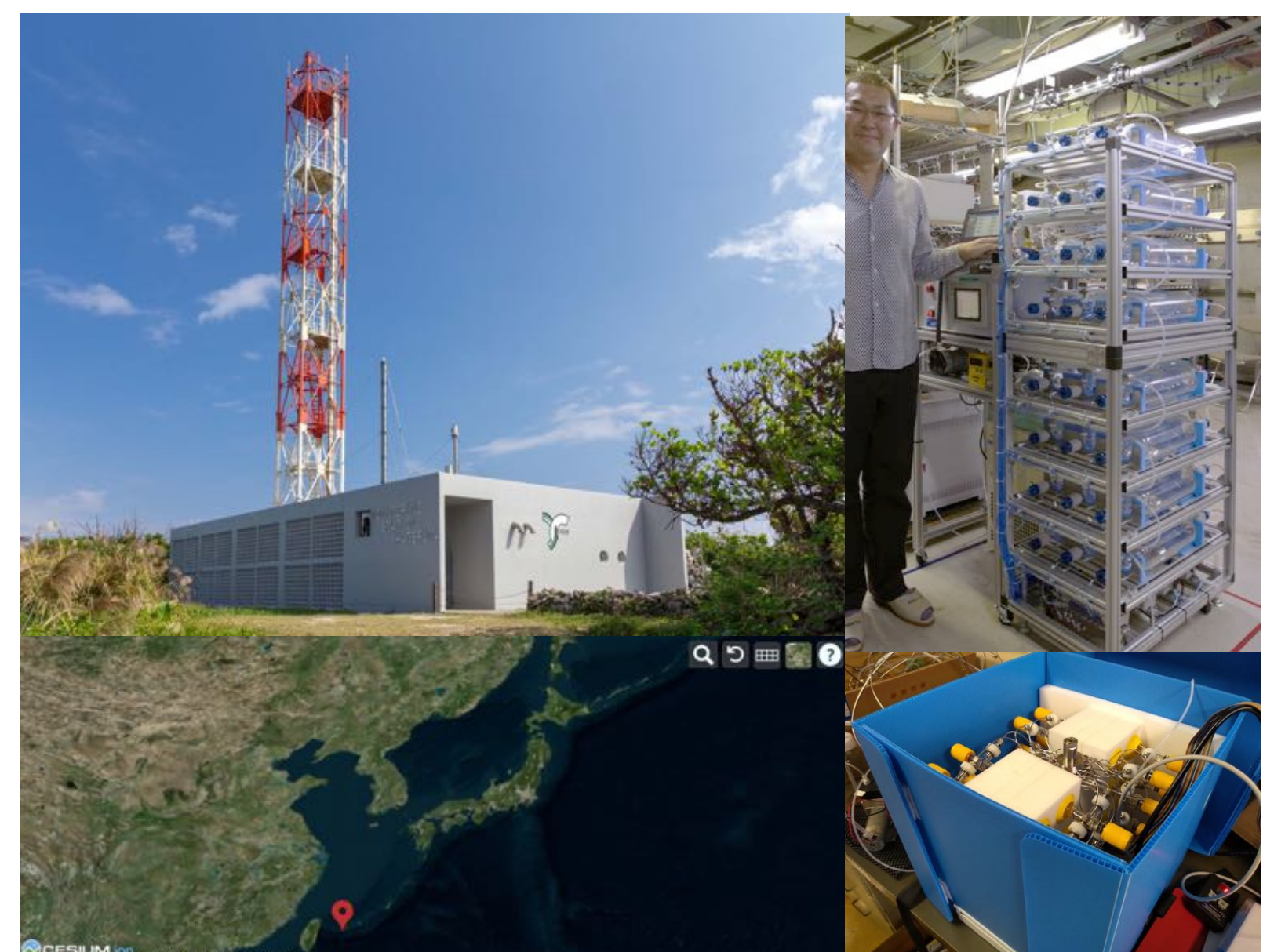


Figure 5. (Left top) A picture of the Hateruma Station (HAT), Japan (<https://esd.nies.go.jp/ja/about/facilities>). (Left bottom) Location of HAT (red icon, <https://db.cger.nies.go.jp/gdi>). (Right top) A picture of the Hateruma event sampler (HEV). This sampler collects sample air into series of ~2.5 L glass flasks at pre-scheduled timings. (Right bottom) A picture of the compact air sampler (CASPER). This sampler houses series of ~0.1 L glass flasks. The sampler switches automatically and post-decision samplings are made, referring to in-situ CH<sub>4</sub> measurement.

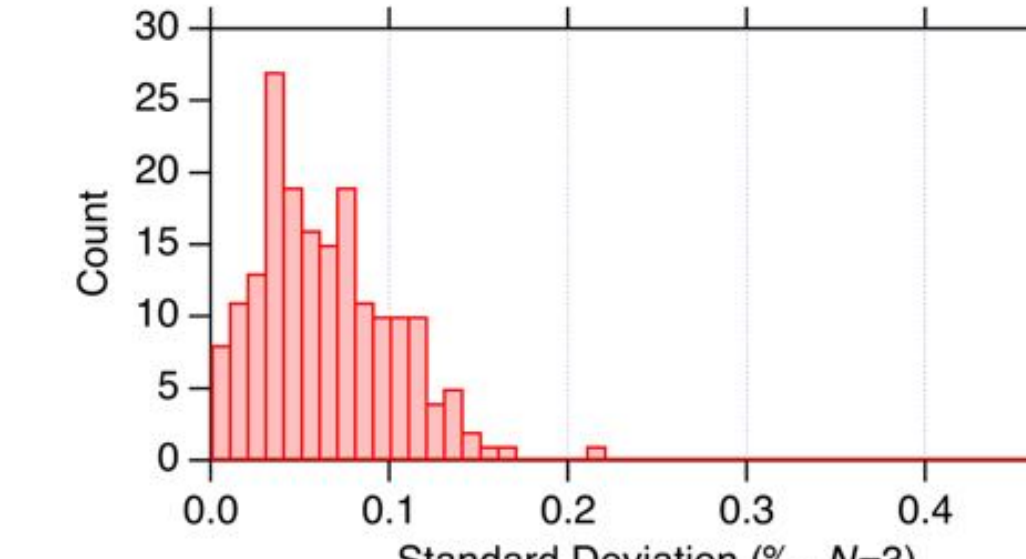


Figure 6. A histogram of the standard deviation from the three-times analyses of the HEV samples (183 samples in total). More than 80% of the sample measurements showed standard deviations of < 0.1‰.

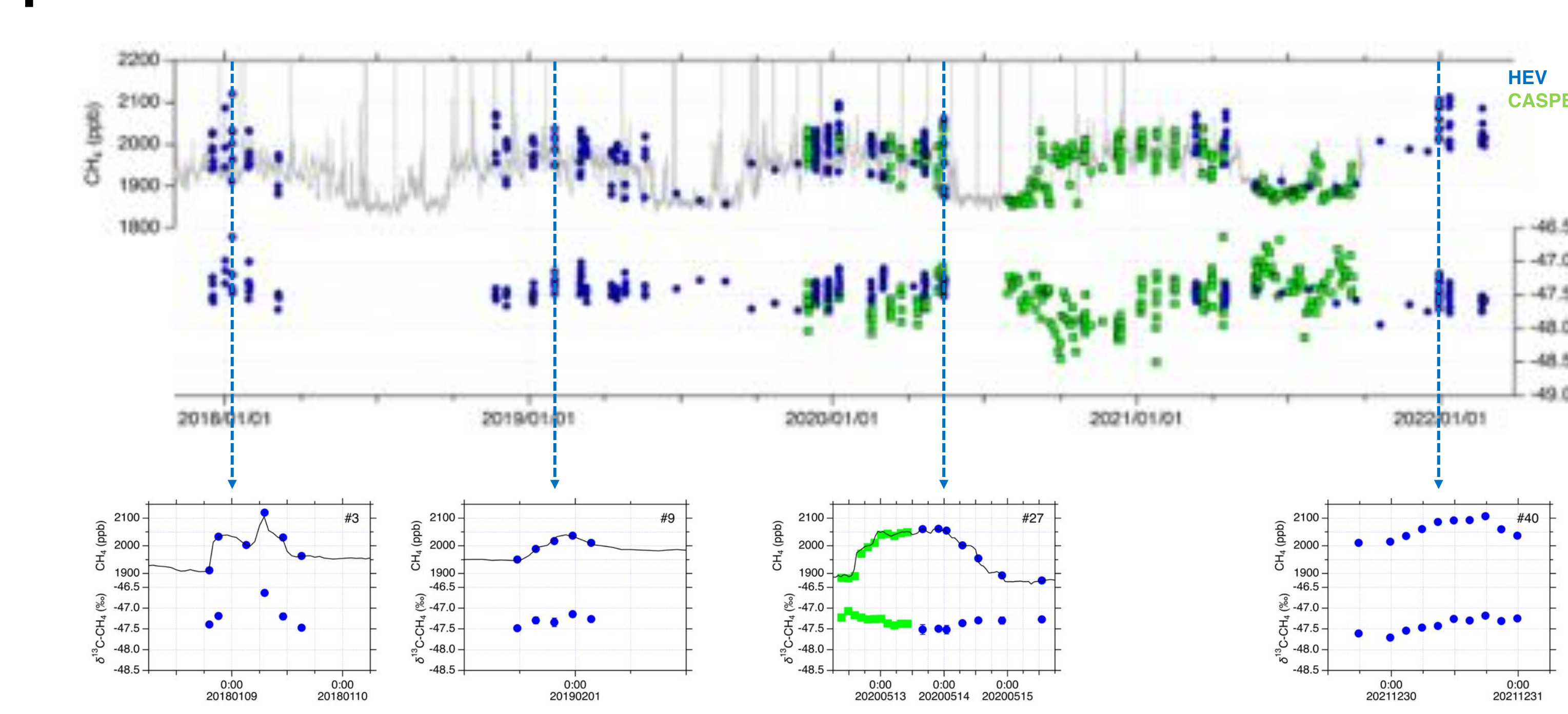


Figure 7. Time series of the CH<sub>4</sub> mole fraction (top panel, left axis) and  $\delta^{13}\text{C-CH}_4$  (top panel, right axis) at HAT. Grey line shows the in-situ CH<sub>4</sub> measurements at 1-hour intervals ([Tohjima et al., 2002](#)). The measurement results from the two samplers HEV and CASPER (see Figure 5) are shown by blue and green symbols, respectively. Zoom-in figures for selected high-CH<sub>4</sub> events are also shown (bottom panels).

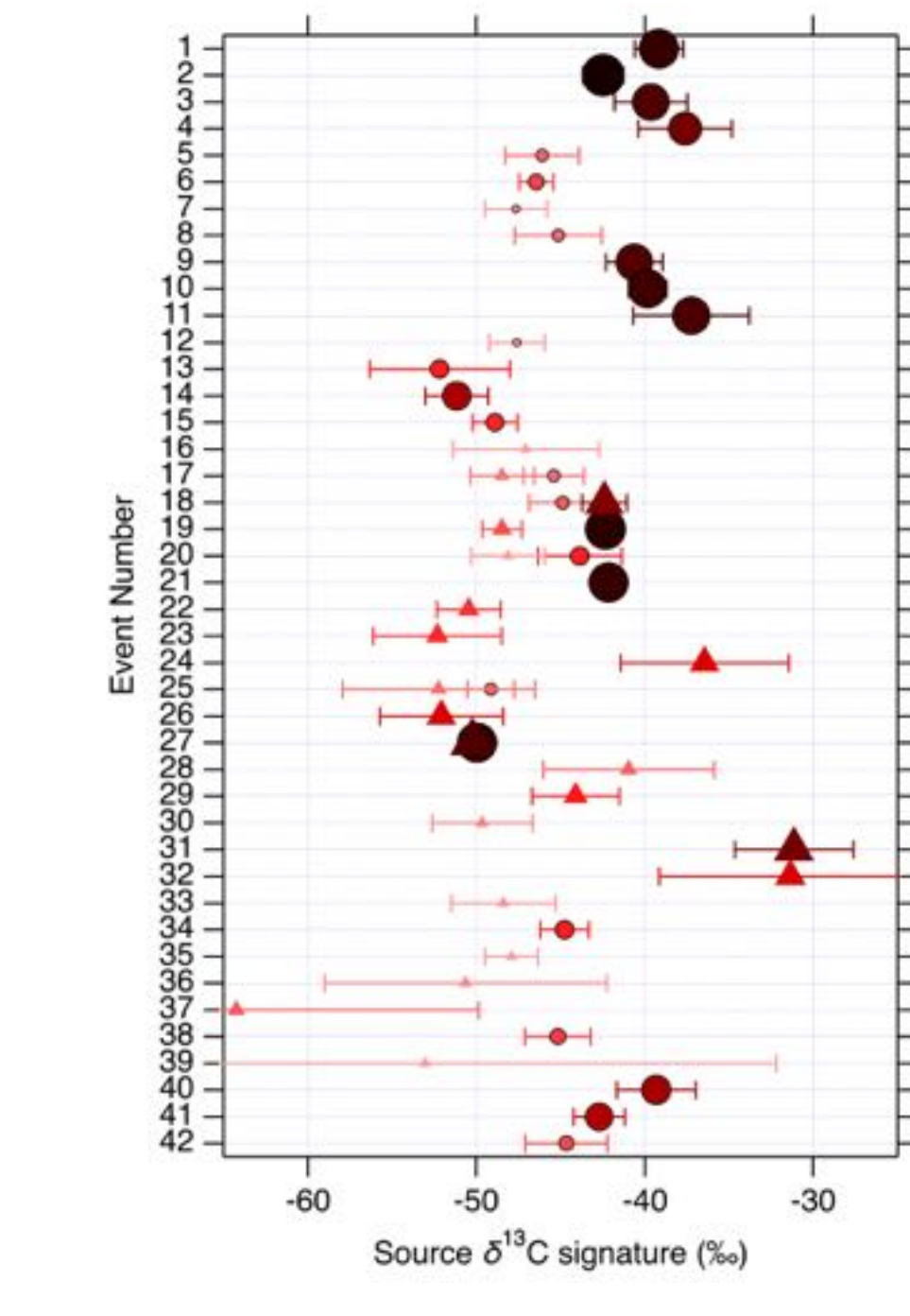


Figure 8. The  $\delta^{13}\text{C-CH}_4$  source signatures inferred from Keeling plots for high-CH<sub>4</sub> events at HAT. Dark and large symbols indicate high correlation coefficients between CH<sub>4</sub> mole fraction and  $\delta^{13}\text{C-CH}_4$ . Circles and triangles are from HEV and CASPER, respectively.